2016-2017 Central Italy Earthquake: Seismic Assessment of "Pietro Capuzi" School in Visso (Marche)

†*Chiara Ferrero[1], Paulo B. Lourenço[2], and Chiara Calderini[1]

[1]Department of Civil, Chemical and Environmental Engineering (DICCA), University of Genoa, Genoa, Italy.
[2]ISISE, Department of Civil Engineering, University of Minho, Guimarães, Portugal.

*Presenting author: chiara.ferrero@edu.unige.it
†Corresponding author: chiara.ferrero@edu.unige.it

Abstract

A prolonged seismic sequence struck the regions of Central Italy between August 2016 and January 2017, causing several fatalities and widespread damage to the built environment. The main objective of this work was to study the structural and seismic behavior of “Pietro Capuzi” school, located in Visso, in the Marche region, which was severely damaged by the 2016-2017 Central Italy Earthquake. A 3D finite element (FE) model of the entire school was prepared, adopting a macro-modelling approach to represent masonry materials. An eigenvalue analysis was initially performed in order to identify the dominant modes of vibration of the structure and calibrate the numerical model according to the results of the dynamic identification tests. Afterwards, non-linear static analyses were performed on the calibrated FE model to evaluate the seismic response of the structure. Finally, the numerical results obtained in terms of failure mechanisms and seismic capacity were compared with the real damage experienced by the building. The numerical model proved to accurately predict the seismic response exhibited by the structure during the past seismic events.

Keywords: **Unreinforced masonry, finite element modeling, seismic assessment, non-linear analysis**

Introduction

Recent and past earthquakes have shown that unreinforced masonry buildings are prone to damage by seismic actions. However, the seismic assessment of such structures is a highly demanding task, not only for the potential complexity of this kind of buildings, but also for the lack of data usually available regarding geometry, construction details and material mechanical characterization. This study was aimed at assessing the seismic performance of “Pietro Capuzi” school, located in the municipality of Visso (Marche, Italy), which was severely damaged by the 2016-2017 Central Italy earthquake, also named the Amatrice-Visso-Norcia seismic sequence. The school was an excellent case study to investigate the seismic capacity of an existing masonry structure for several reasons. Firstly, “Pietro Capuzi” school is part of the public buildings permanently monitored by the Seismic Observatory of Structures (hereafter named OSS). As a result, the entire seismic sequence affecting the structure was recorded by the existing system of accelerometers [1], thus providing valuable information in terms of seismic input at the base as well as vibrations experienced at different levels. Secondly, the inspection and extensive experimental campaign that were performed in 2011 on behalf of the OSS supplied detailed documentation regarding geometry, structural configuration, construction details as well as some information about the mechanical properties of masonry [2][3][4]. Furthermore, dynamic identification tests were also carried out in 2011 to characterize the dynamic response of the structure [5]. Such documentation, acquired from the OSS, was integrated with the information about geometry, structural configuration, past interventions and seismic damage supplied by the Italian Network of

University Laboratories in Seismic Engineering (RELUIS) and the University of Genova, in charge of post-earthquake surveys [6][7]. In addition, the photographic record of the progressive damage experienced by the building during the entire seismic sequence was provided by the Italian Department of Civil Protection [8]. In conclusion, the availability of such detailed data, which is not very common, allowed for the preparation of a detailed FE model of the entire structure. This was then updated on the basis of the modal parameters determined experimentally by the OSS. Furthermore, the detailed description of the damage experienced by the structure during the entire seismic sequence provided the opportunity to validate the numerical model of “Pietro Capuzi” school through a comparison between the damage simulated and the damage pattern observed.

Description of the building

Overall configuration and use

Built in the 1930s, "Pietro Capuzi" nursery and primary school (Figure 1) is a stand-alone structure located in the urban area of Visso, in the Marche region. The building has four levels, three of them above ground (raised ground floor, first floor and attic) and a basement partially sub-grade (Figure 1c). The three levels above ground have a plan area of approximately 605 m^2 each, whereas the basement has a plan area of approximately 120 m^2. The basement, raised ground floor and first floor have an inter-storey height of 3.09 m, 4.44 m and 4.26 m respectively. The attic has a maximum height of about 3.19 m, resulting in a total height above ground of about 13.50 m in correspondence of the main façade. The total built volume is estimated at about 4800 m^3.

The building does not present any narrowing or enlargement of the horizontal section along the height in the part above ground. However, it is strongly irregular in plan since it presents a T-shape configuration given by the connection of two orthogonal bodies (hereafter named Body A and Body B as shown in Figure 1b). Body A, characterized by an elongated rectangular shape and oriented in NW-SE direction (hereafter called X direction as indicated in Figure 1b), hosts most of the classrooms, while the areas used as offices, the canteen and toilets are allocated in Body B. A staircase connecting the basement, raised ground floor and the first floor is located on the east side of Body B.

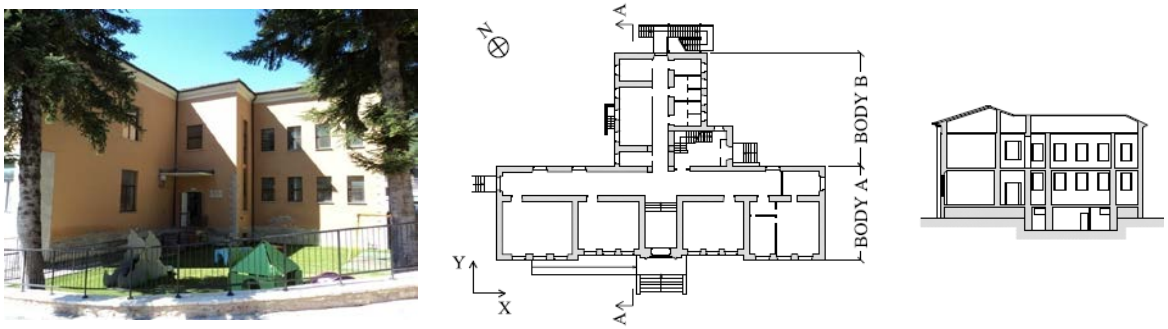

(a) (b) (c)

Figure 1 – “Pietro Capuzi” school: (a) external view, (b) plan of the raised ground floor, and (c) section AA [2].

Structural configuration and technical details

The structure of the building consists of load-bearing masonry walls that extend upwards from the basement until the attic. The prevalent type of masonry is a stone masonry, whereas

the sporadic presence of solid brick masonry can be observed in some pillars in the staircase as well as in portions of walls filled with solid bricks during past interventions. The thickness of the walls varies with height, ranging from about 70-85 cm at the basement to approximately 70 cm at raised ground floor and 50-70 cm at first floor. Foundations are made of the same stone masonry of the upper levels that extend downwards until a depth of approximately 60 cm from the planking level of the basement.

Concerning horizontal diaphragms, the slabs of the raised ground floor and first floor are lightweight slabs, with a thickness of 30 cm each, while the slab between first floor and the attic is a steel-clay slab. In the areas of the raised ground floor where there is no basement, the slab on grade consists of a concrete slab resting directly on the ground. The staircase is made of reinforced concrete, and it is supported on load-bearing masonry walls on three sides, and three masonry pillars on the internal short side. The hipped roof has a timber structure consisting of purlins and rafters that are supported by a system of trusses or by the inner walls extending until the top of the roof. In correspondence of ridges and valleys, hip rafters are present. Above the timber structure, clay tiles are located. A reinforced concrete bond beam is located at the height of the spring line of the roof.

Past damage and previous strengthening interventions

"Pietro Capuzi" school was damaged by the seismic events that hit the regions of Umbria and Marche between 1997 and 1998. Cracks mainly appeared in the staircase where the two bodies composing the building connect to each other. This led to a strengthening intervention performed in the 1990s, which was aimed at: (1) repairing the seismic damage, (2) improving the seismic capacity of the building, and (3) solving static problems due to the decay of some parts of the timber roof. As for the latter, the original roof timber structure was replaced with new glue laminated timber elements in the central part of Body A above the classrooms. As for the seismic damage, the major cracks were repaired using the technique of "cuci and scuci". Regarding the seismic improvement, the interventions carried out included: (1) addition of metallic profiles studded to the internal side of masonry walls at the height of the slab between first floor and attic, (2) connection of the roof timber elements to the perimeter walls by means of metallic plates anchored with bars, (3) creation of a steel frame around the openings of the main façade at the first level, (4) addition of metallic tie-rods, (5) injections of lime mortar in some piers where pipes were filled in the past with solid brick masonry, and (6) filling with solid brick masonry of the spans between the pillars in the staircase.

Seismic damage and monitoring data

The 2016-2017 Amatrice-Visso-Norcia seismic sequence started on August 24th, 2016 with the Amatrice earthquake (M_w 6.0), which hit a vast area of the Central Apennines producing almost 300 casualties and widespread damage to the built environment. The sequence was characterized by nine mainshocks with moment magnitudes higher than 5, which occurred on August 24th, 2016 (M_w 6.0 and M_w 5.4), October 26th, 2016 (M_w 5.4 and M_w 5.9), October 30th, 2016 (M_w 6.5) and January 18th, 2017 (four shakes with $M_w \geq 5.0$).

Damage suffered in the 2016-2017 Amatrice-Visso-Norcia seismic sequence

"Pietro Capuzi" school suffered severe damage due to the Amatrice-Visso-Norcia seismic sequence. A detailed description of the damage experienced by the building, updated on the date of December 8th, 2016, was reported in [6][7]. As shown in Figure 2a, the walls were affected by severe cracks at both the raised ground floor and first floor, especially in the Y direction where the damage is more severe and widespread than in the X direction. The building mainly presents diagonal shear cracks developing through the entire thickness of the

walls in both piers and spandrels. Furthermore, a shear-sliding mechanism producing an important residual deformation was activated in the northwest (NW) side of the building (Figure 2b). Flexural cracks can also be observed on the southeast (SE) side of Body B (Figure 2c). In addition to the in-plane damage, an out-of-plane mechanism occurred in the NW corner of the building, resulting in the partial collapse of the masonry walls and adjacent attic slabs (Figure 2d).

With regards to the other slabs, two local collapses occurred in the slab between the raised ground floor and first floor (Figure 2e). Furthermore, the steel slab between first floor and attic experienced an extensive collapse because of the out-of-plane mechanisms as well as cracks along the metallic profiles in the portions of slab still standing. For the connection between vertical walls and slabs, horizontal cracks were present in the external walls at the slab locations. In the interior, severe cracks were observed in correspondence of the connection between walls and slabs (Figure 2f).

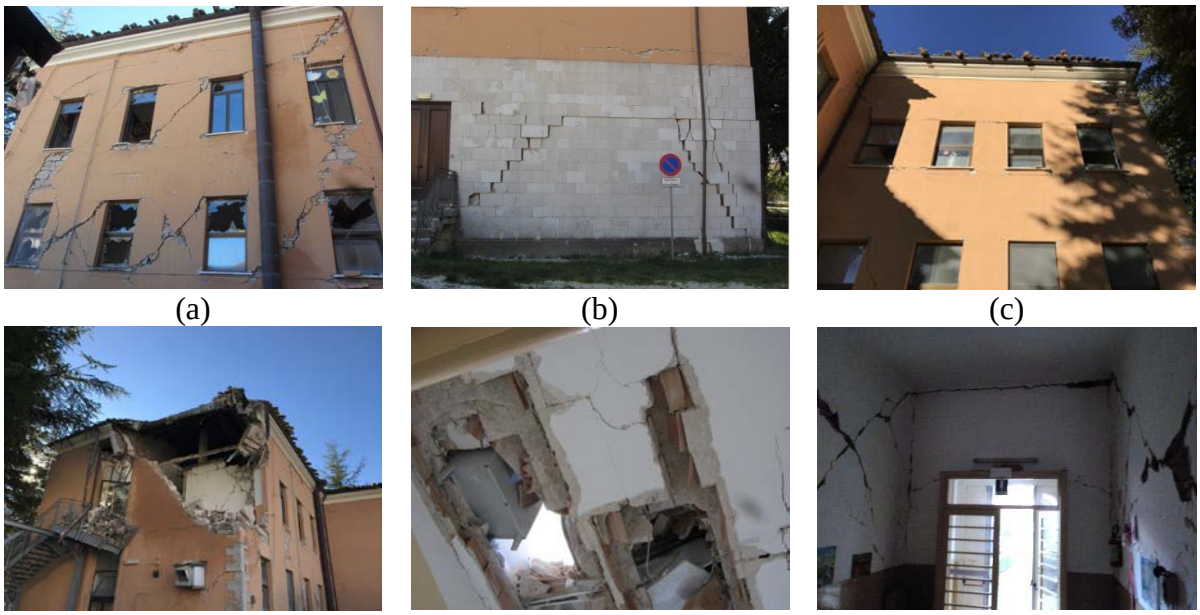

Figure 2 – Damage state updated on December 8th, 2016: (a) diagonal shear cracks in piers and spandrels, (b) shear-sliding mechanism, (c) out-of-plane mechanism, (d) flexural cracks, (e) local collapse of the slab between raised ground floor and first floor, (f) cracks in correspondence of the connection between walls and slabs [6].

A partial reconstruction of the damage development experienced by “Pietro Capuzi” school during the Amatrice-Visso-Norcia seismic sequence was carried out thanks to the photographic documentation provided in [8]. After the seismic event of August 24th, the building exhibited an in-plane response with cracks occurring in both masonry piers and spandrels (Figure 3a). In addition to moderate cracks widespread throughout the entire building, severe cracking appeared in some piers of internal and external walls. As shown in Figure 3b, the earthquakes that occurred on October 26th, 2016 produced significant deterioration of the damage level. Not only did the severity of the in-plane damage increase significantly, but an out-of-plane mechanism also occurred. As for the in-plane response of masonry walls, it was observed than, more than in the creation of new cracks, the deterioration of the damage state mainly consisted in the enlargement of the cracks produced by the seismic event of August 24th. As shown in Figure 3c, the damage state did not change significantly after the shake of October 30th with respect to October 26th.

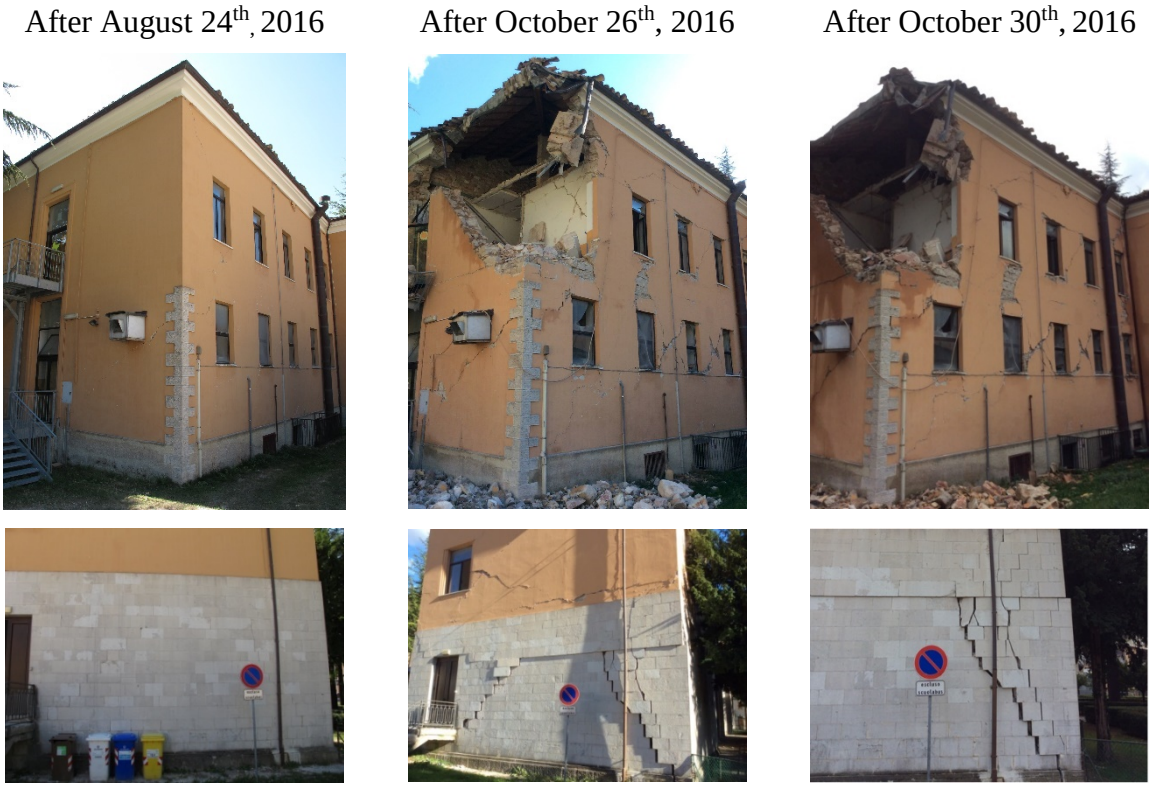

Figure 3 – Observed damage in "Pietro Capuzi" school after the earthquakes occurred on: (a) August 24th, 2016, (b) October 26th, 2016, and (c) October 30th, 2016 [8].

Permanent Monitoring by the Seismic Observatory of Structures

As part of the OSS, "Pietro Capuzi" school is permanently monitored by a system of accelerometers located in different parts of the structure: one tri-axial accelerometer is located in the basement to measure the seismic input, and ten bi-axial accelerometers are placed at the first and second levels at the intrados of the slabs to record the accelerations experienced by the structure. For all of these sensors, the OSS provided the authors with the time histories in acceleration and displacement obtained for the seismic events occurred on August 24th (M_w 6.0), October 26th (M_w 5.4 and 5.9) and October 30th (M_w 6.5) [1][6]. These recordings allowed characterization of the seismic input at the base of the structure and aided in drawing significant conclusions about the accelerations experienced by the building.

For the four seismic events considered, Table 1 reports the distance of the epicenter from "Pietro Capuzi" school as well as the values of the peak ground acceleration (PGA) obtained for the two horizontal components XX and YY, and vertical component ZZ. The structure was subjected to significant values of horizontal ground motion, in particular the highest values of horizontal PGA were recorded during the M_w 5.9 earthquake of October 26th, which are equal to 0.36 g and 0.47 g in the XX and YY directions, respectively.

Table 1 – Distance from the epicenter and PGA for the seismic events of August 24th, October 26th and October 30th.

Seismic event	Distance from epicenter [km]	PGA x [g]	PGA y [g]	PGA z [g]
2016/08/24_M_w = 6.0	28	0.33	0.32	0.14
2016/10/26_M_w = 5.4	7	0.30	0.21	0.41
2016/10/26_M_w = 5.9	4	0.36	0.47	0.31
2016/10/30_M_w = 6.5	10	0.29	0.30	0.33

Figure 4 shows a comparison between the 5% damped acceleration response spectra of the horizontal components of motion in XX and YY directions for the four earthquakes considered, and the elastic response spectrum in accordance with the Italian Building Code (hereafter called NTC2008 [9]) for a return period of 712 years and soil of type B [3]. It is observed that the seismic events of August 24th (M_w 6.0) and October 26th (M_w 5.9), which caused the most severe damage to the structure, resulted in significant amplifications of the acceleration with respect to the elastic spectrum of NTC2008. Furthermore, it is important to note that the YY component of the acceleration spectrum of October 26th earthquake exceeded the code spectrum for all the significant ranges of period, thus agreeing with the severe damage suffered by the structure in this direction.

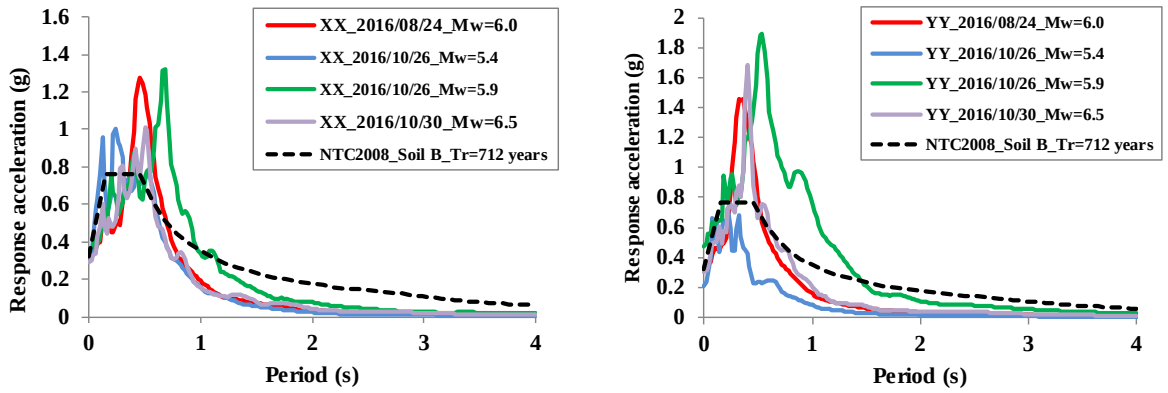

Figure 4 - Comparison between the response spectra (XX and YY component) of the seismic events of August 24th, October 26th and October 30th and the elastic spectrum of NTC2008 for soil B and return period Tr=712 years (damping 5%).

The monitoring system installed in the school provided useful information to characterize the seismic performance of the building during the entire seismic sequence. Table 2 reports the values of the maximum acceleration recorded on the structure (PSA), the amplification factor ($\alpha_{PSA/PGA}$, calculated as the ratio between PSA and PGA), and the maximum inter-storey drift (Dmax, i.e. the maximum ratio of the relative floor displacement to the height of the corresponding floor), for the seismic events on August 24th (M_w 6.0), October 26th (M_w 5.4 and 5.9) and October 30th (M_w 6.5). First, it was observed that the structure underwent values of acceleration that were significantly amplified with respect to the maximum acceleration measured at the base. Indeed, very high values of amplification factors, even higher than 4, were obtained. Furthermore, some interesting observations could be drawn analyzing the values of inter-storey drift produced during the seismic sequence. With this aim, the OSS

already provided the following reference values regarding drift-damage relation for masonry buildings: (1) no damage for drift ranging from 0 to 2‰, (2) slight damage for drift ranging from 2‰ to 4.5‰, (3) moderate damage for drift ranging from 4.5‰ to 8‰, and (4) severe damage for drift higher than 8‰ [10]. The highest values of drift were produced by the M_w 5.9 earthquake of October 26th, for which values of 13.53 and 16.01 were obtained in X and Y direction respectively. These values were significantly higher than the ones resulting from the shakes of August 24th and October 26th (M_w 5.4). According to the reference values provided by OSS, the values of drift obtained for the M_w 5.9 earthquake of October 26th corresponded to serious damage, while moderate and slight damage were respectively associated to the shakes of August 24th and October 26th (M_w 5.4). Note that the values of drift obtained for the M_w 6.5 earthquake of October 30th were less meaningful since the building had been severely damaged by the previous seismic events. These results were consistent with the damage level exhibited by the building during the entire seismic sequence. Furthermore, the higher values of drift obtained in the Y direction for the seismic events of October agree with the more severe damage observed in the structure in the Y direction with respect to the X direction. Consequently, the inter-storey drift was found to represent a reliable measure of the damage suffered by the structure after the earthquake.

Table 2 – Parameters characterizing the seismic response of the structure for the seismic events of August 24th, October 26th and October 30th.

Seismic event	PSA x [g]	PSA y [g]	$\alpha_{PSA/PGA,x}$	$\alpha_{PSA/PGA,y}$	Dmax x [‰]	Dmax y [‰]
2016/08/24_M_w = 6.0	1.05	0.80	3.21	2.52	6.10	4.23
2016/10/26_M_w = 5.4	1.27	0.78	4.27	3.70	3.95	2.46
2016/10/26_M_w = 5.9	1.41	1.33	3.86	2.81	13.53	16.01
2016/10/30_M_w = 6.5	1.36	1.47	4.65	4.89	5.52	10.98

Numerical model

Preparation of the FE model

A 3D finite element (FE) model of “Pietro Capuzi” school was created in Midas FX+ Version 3.3.0 Customized Pre/Post-processor for DIANA software [11]. A macro-modelling approach was used to represent masonry, which was considered as a composite material without any distinction between units and mortar [12]. Geometry definition is essential when dealing with the modeling of a complex structure [13] since any adopted strategy may entail different final results. “Pietro Capuzi” school has three levels above the ground and a basement partially sub-grade. Modeling building portions below ground is often controversial, especially when detailed information about the foundations is not available. Hence, the first decision to be made was the basement modeling strategy, and three different models were considered, as illustrated in Figure 5. As shown in Figure 5a, the basement occupies only a part of the plan area of the first level of Body B. Model A neglects the portion of the basement underground (Figure 5b), whereas model B and C take it into consideration by extending the walls of the basement downwards. The main distinction between models B and C is that the first one considers only the walls where the basement is located according to the geometrical survey (Figure 5c), whereas the second one assumes an equal height underground (1.47m) along all the walls of Body B, in agreement with past modelling strategies [4]. Note that the passive earth pressure exerted on the walls of the basement was not considered due to the limited

height of the portion of the basement underground. The choice of the model to use for structural analyses was based on the comparison between the experimental and numerical responses of the different models in terms of frequencies and mode shapes (see the following paragraph). Note that the three models only differ for the presence of the basement, therefore the description of geometry and materials presented below is applicable to all.

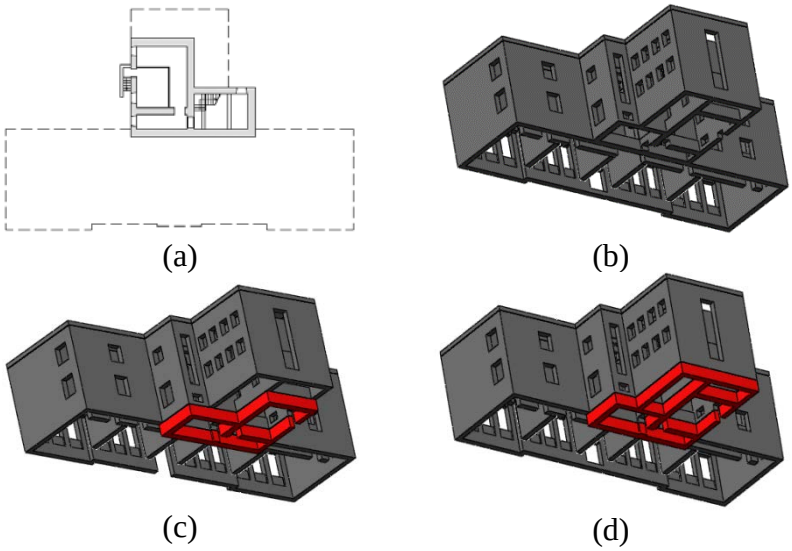

Figure 5 – (a) Plan of the basement, and geometry of the different FE models prepared for the school: (a) model A, (b) model B, (c) model C.

Masonry walls were modeled using solid FEs; in particular, four-node three-sided isoparametric solid tetrahedron elements (TE12L) were adopted [11]. Although the use of shell elements for the walls would have resulted in a significant reduction of the number of degrees of freedom and, consequently, a more limited computational effort, the strategy of using solid FEs was adopted because of the presence of masonry panels characterized by a similar length in both axial and transversal directions.

Regarding diaphragms, three-node triangular (T15SH) and four-node quadrilateral (Q20SH) isoparametric curved shell elements were adopted to model the intermediate slabs [11]. The roof was built as an ensemble of inclined surfaces supported by masonry walls (Figure 6a). Since a detailed survey of the roof timber structure was not available, it was believed that this solution might allow an adequate load distribution on the perimeter walls. In the case of the roof, only three-node triangular isoparametric curved shell elements were used to assure a better-quality mesh and prevent the creation of elements with undesirable shapes in the corners.

Finally, 1D elements were used to model beams and tie-rods. Two-node, three-dimensional class-I beam elements (L12BE) were adopted for the reinforced concrete beams located at the entrance and in the staircase as well as the reinforced concrete bond-beam present at the top of the building. Two-node regular directly integrated (1-point) truss elements (L2TRU) were adopted to mesh metallic tie-rods [11].

The geometry and final mesh of the school are shown in Figure 6 for model B. In total, the numerical model is composed by 180.567 nodes and 696.997 elements in the case of model A, 187.988 nodes and 727.853 elements as for model B, and 189.256 nodes and 730.953

elements in the case of model C. Regarding the boundary conditions, a clamped boundary condition was adopted at the base of the walls, and all the degrees of freedom were restrained.

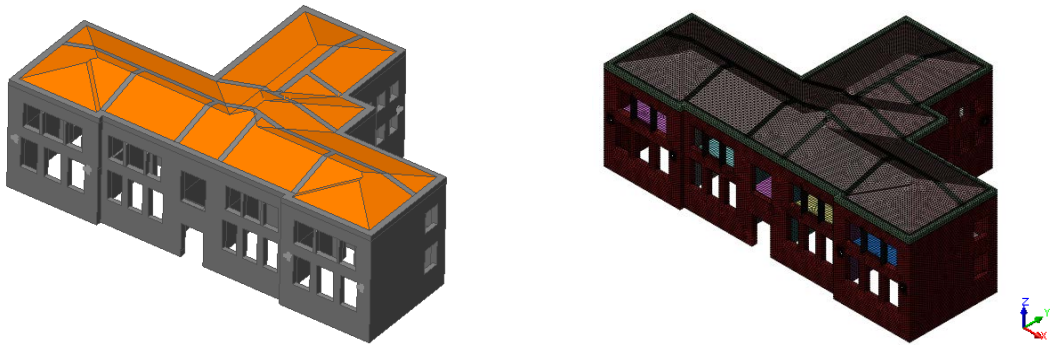

(a) **(b)**

Figure 6 – Three-dimensional model: (a) geometry and (b) mesh discretization.

Material and diaphragm properties

A description of the properties adopted for materials and diaphragms is presented below. To perform numerical analyses, a non-linear behavior was adopted exclusively for masonry materials, whereas a linear elastic behavior was employed for slabs, reinforced concrete beams and tie-rods. The physical non-linear behavior of masonry was simulated by means of the Total Strain Rotating Crack Model that is available in DIANA [11]. To represent masonry behavior in tension and compression, an exponential stress-strain relationship and a parabolic stress-strain relationship were adopted, respectively. Three different types of masonry were identified in the building and represented in the FE model: (1) cut stone masonry with good texture, (2) stone masonry injected during past interventions, and (3) solid brick masonry.

The physical and mechanical properties of the different types of masonry adopted in the numerical model are reported in Table 3. The elastic properties of masonry materials were defined according to the prescriptions given by the Italian Circolare for knowledge level LC2 [14], considering also the qualitative and quantitative information obtained from past inspections and tests [3][6]. Some corrective coefficients, as indicated in [14], were adopted to improve the properties of stone and brick masonry due to the presence of injections and good mortar, respectively. As for the inelastic properties, they were determined on the basis of information and recommendations available in literature [15][16].

Table 3 - Material properties of the different types of masonry adopted in the numerical model.

Material property	Stone masonry	Stone masonry (+ injections)	Brick masonry (+ good mortar)
Specific weight [kN/m^3]	21	21	18
Elasticity modulus [MPa]	1740	2610	2250
Poisson's ratio [-]	0.2	0.2	0.2
Compressive strength [MPa]	2.67	4.00	4.00
Compressive fracture energy [N/mm]	4.27	6.40	6.40
Tensile strength [MPa]	0.108	0.163	0.190
Tensile fracture energy [N/mm]	0.024	0.024	0.024

The physical and mechanical properties adopted for reinforced concrete and steel are presented in Table 4. Since no physical or mechanical characterization was available, the properties of these materials were derived from NTC2008 [9].

Table 4 – Material properties of reinforced concrete and steel.

Material property	Concrete	Steel
Specific weight [kN/m^3]	25	78.5
Modulus of elasticity [MPa]	31500	210000
Poisson's ratio [-]	0.2	0.29

Regarding the slabs, the only properties to determine were bending and axial stiffness since a linear elastic behavior was adopted for them. These properties are automatically calculated in DIANA on the basis of the elasticity modulus of the material assigned to the slabs and the thickness of the FEs (curved shell elements in this case) used to model them. In this study, the values of an equivalent modulus of elasticity E_{eq} and an equivalent thickness h_{eq} to input in DIANA were calculated based on the real bending and axial stiffness of a strip of slab as wide as the spacing between the principal elements composing the slab structure.

An isotropic or orthotropic material was adopted for two-way and one-way slabs, respectively. For the former, the same value of stiffness was adopted in the two in-plane directions, whereas for the latter, stiffness equal to the 10% of the principal direction was assumed in the secondary direction. As for the stiffness in the orthogonal direction (vertical direction), it was estimated so that it fulfilled the requirements of orthotropic elasticity reported in [11].

Table 5 presents the in-plane axial stiffness in both principal and secondary directions (E_1h and E_2h) and the bending stiffness in the vertical direction ($E_3h^3/12$) for the different types of slabs.

Table 5 - Properties of diaphragms adopted in the numerical model.

Type of diaphragm	Type of material	E_1h (kN/m)	E_2h (kN/m)	$E_3h^3/12$ (kNm)
Lightweight concrete slab (one-way)	orthotropic	3.001E+06	3.001E+05	7.051E+03
Lightweight concrete slab (two-way)	isotropic	2.644E+06	2.644E+06	1.061E+04
Steel slab (one-way)	orthotropic	3.822E+05	3.822E+04	6.618E+02
Roof	isotropic	1.889E+06	1.889E+06	5.666E+02

Eigenvalue analysis and model updating

A first eigenvalue analysis was carried out to obtain the natural frequencies and modes shapes of the three different models prepared for “Pietro Capuzi” school. In order to identify which model better simulated the real behavior of the structure, the numerical results were compared with the ones derived from the dynamic identification tests performed by [5] in terms of natural frequencies and mode shape. The OSS provided the natural frequencies as well as the mode shape vectors for three vibration modes. For these modes, the deformed shape, shown

in Figure 7a for the first level of the building, was obtained in this study by drawing in scale on the plan of the building the modal displacements associated to each mode shape vector. The modes identified experimentally were global modes corresponding to: (1) a translational mode in the transversal direction of the building (mode 1 - 3.175 Hz), (2) a torsional mode (mode 2 - 3.755 Hz), and (3) a translational mode in the longitudinal direction (mode 3 - 4.047 Hz).

In order to gather more information about the modal response of the structure and visualize animations of the mode shapes, a further dynamic identification was performed in ARTeMIS Modal 5.0 software [17] by processing the signals recorded by [5] during the dynamic tests carried out in 2011. Though richer in terms of more possible frequencies, this dynamic identification whose results are reported in [18], was consistent with the one carried out by [5]. The latter was used by the authors to perform the updating of the numerical model. Hence, the model updating was focused on the three modes identified in [5], which were compared with the ones obtained numerically that presented a similar mode shape (Figure 7b). Note that only the mode shapes obtained for model B are presented in Figure 7b due to the similarity of results obtained for the three models.

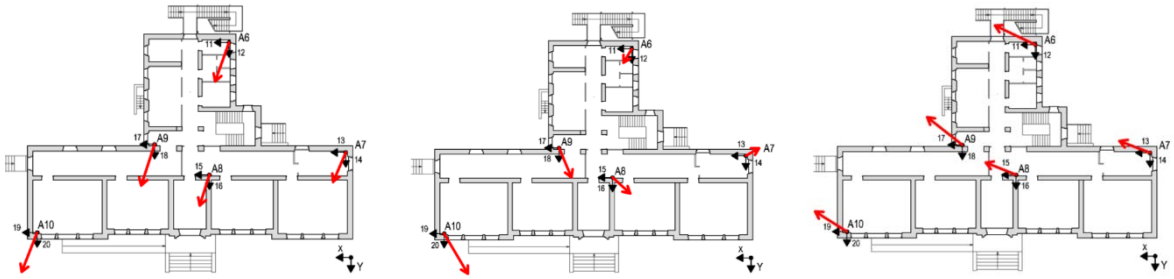

Mode 1 (3.175 Hz) Mode 2 (3.755 Hz) Mode 3 (4.047 Hz)

(a)

Mode 1 (5.57 Hz) Mode 2 (5.77 Hz) Mode 3 (5.92 Hz)

(b)

Figure 7 - Mode shapes obtained (a) experimentally and (b) numerically (for model B).

Subsequently, for the three global modes identified, a comparison between numerical and experimental results was performed in terms of frequency error and modal assurance criterion (MAC). The latter is a statistical indicator that is normally used to compare the mode shapes obtained from analytical or numerical models with the ones obtained experimentally [19].

Table 6 presents the average frequency errors and MACs for the three models. A similar frequency error of about 60%, calculated on average between the frequencies of the three modes, was obtained for the three different models. As for the average of MACs, the value obtained for model C (0.53) was much lower than the ones obtained for model A (0.68) and model B (0.69). Since the average frequency error was slightly lower for model B (58.5%)

when compared with model A (59.8%), model B was considered the model that better simulates the real behavior of the structure, and it was used for model updating and further structural analyses.

Table 6 - Comparison of numerical and experimental frequencies and mode shapes

	Model A	Model B	Model C
Average frequency error [%]	59.8	58.5	56.2
Average MAC	0.68	0.69	0.53

As shown in Table 6, the average of the frequency errors for model B is significantly high, consequently model updating was necessary to calibrate the numerical model of the school. Two different strategies of model updating were adopted considering different parameters as variables to tune and using an iterative procedure in order to minimize frequency error and MAC.

Table 7 presents the results obtained for the two calibrations carried out. The first calibration was performed adjusting the properties of masonry materials and diaphragms. Concerning masonry materials, the elasticity modulus of stone and brick masonry was considered for the updating process. As for the slabs and roof, the axial stiffness was varied while keeping the bending stiffness constant. However, this last strategy was disregarded since considerable reductions of the axial stiffness of the diaphragms produced only limited decreases in the values of the numerical frequencies, but, at the same time, resulted in a sharp decrease of the average MAC. On the other hand, since the natural frequencies obtained numerically were significantly higher than the experimental ones, a sharp reduction of the initial values adopted for the elasticity modulus of masonry was needed to reach a reasonable average frequency error of about 6%. The latter was derived considering an elasticity modulus of 700 MPa, 1050 MPa and 905 MPa respectively for stone masonry, stone masonry with injections and brick masonry. Although these values were still within the range of values provided by the Italian Circolare [14], such a significant reduction may indicate that masonry was poorly built, was damaged when the dynamic tests were performed, or soil conditions significantly influenced the measures of frequency values. For these reasons, a further calibration was carried out considering soil-structure interaction and adopting a finite stiffness for the soil.

To model the soil, plane interface elements (T18IF [11]) were placed at the base of the walls in the numerical model. The values of normal stiffness modulus k_n and shear stiffness modulus k_t that must be input for the interfaces were adopted as the variable to update. On the basis of the values of dynamic Young's modulus and dynamic shear modulus of the soil (as reported in [3]), the reference values of the normal stiffness modulus and shear stiffness modulus of the interfaces were assumed as 1.91E+05 kN/m^3 and 6.83E+04 kN/m^3, respectively. A new eigenvalues analysis was performed on the numerical model with interfaces at the base. Model updating was then carried out adjusting the values of normal and shear stiffness moduli of the interfaces until achieving an error between experimental and numerical frequencies lower than 5% for both each mode and on average. Such an error was obtained adopting a value of 1.32E+05 kN/m^3 for the normal stiffness modulus and a value of 4.71E+04 kN/m^3 for the shear stiffness modulus.

Table 7 – Results obtained from different updating strategies.

Updating variables	Frequency error [%] Mode 1	Mode 2	Mode 3	MAC Mode 1	Mode 2	Mode 3	Average f. error [%] All modes	Average MAC All modes
$E_{masonry}$ reference values	75.2	53.0	47.2	0.73	0.77	0.59	58.5	0.70
$E_{masonry}$ updated values	13.5	-1.3	-3.5	0.73	0.79	0.63	6.1	0.72
k_n, k_t interfaces reference values	14.4	5.2	6.1	0.88	0.57	0.70	8.6	0.72
k_n, k_t interfaces updated values	4.3	-2.8	-2.0	0.89	0.55	0.71	3.1	0.72

According to the results reported in Table 7, it can be concluded that the average of MACs is almost insensitive to the updating strategy employed, whereas the model updating based on the stiffness of interfaces resulted in a better matching between the natural frequencies obtained experimentally and numerically. Not only is the error, on average, almost the half of the one obtained by updating the elasticity modulus of masonry, but the error in the frequency of the first mode also comes down to a value of 4.3%, which is significant lower that the 13.5% reached with the first calibration.
In conclusion, the calibrated FE model with interfaces was chosen to perform further structural analyses. For this model, Figure 8 presents the three global mode shapes obtained numerically and corresponding to the experimental ones.

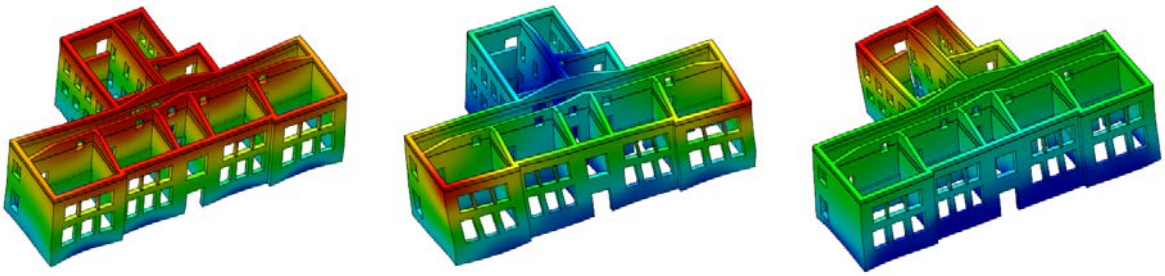

Mode 1 (3.31 Hz) Mode 4 (3.65 Hz) Mode 5 (3.97 Hz)

Figure 8 – Mode shapes of the three global modes obtained for the calibrated model with interfaces.

Non-linear static analyses

Pushover analyses were performed to evaluate the seismic performance of “Pietro Capuzi” school. A lateral distribution pattern proportional to the mass of the structure was adopted to apply horizontal loads. The analyses were performed along the X and Y global axes of the numerical model, corresponding respectively to the longitudinal and transversal directions of the structure, in both positive and negative directions. Eight control nodes, located at the top of the building and characterized by large displacements but small deformations, were used to plot the capacity curves (Figure 9). The damage was associated to high values of principal

tensile strains, which indicated cracking [20]. The principal crack width strain (mm) was also taken into consideration to evaluate the damage state.

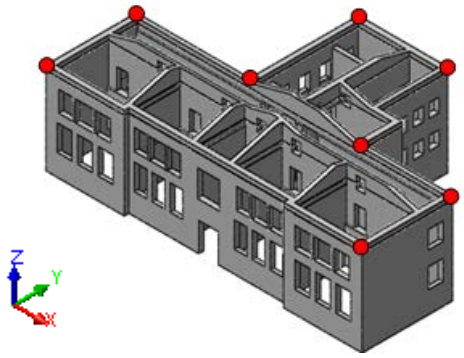

Figure 9 – Control nodes for the pushover analyses.

Figure 10 shows the capacity curves obtained for the pushover analyses performed in +X, -X, +Y and -Y. As for -Y direction, it is important to note that the curve exhibited a long, almost flat, plateau, consistent with a shear or rocking failure mode of masonry elements, without material crushing or geometrical non-linear effects. This made the last point of the curve physically less meaningful, but only related to convergence issues. For this reason, the ultimate capacity of the structure was estimated by taking into consideration the value of ultimate displacement indicated by the Italian Circolare [14] for the verification with respect to ultimate (life safety) limit state for existing masonry buildings. Consequently, the capacity curve presented in Figure 10 was interrupted when the values of ultimate displacement was overcome. Note that the same verification was performed for the analyses carried out in +Y, -X and -X direction, but in these cases the ultimate displacement was not exceeded.

As shown in Figure 10, the building exhibits a higher stiffness and lateral load-carrying capacity in X direction than in Y direction. The maximum values of lateral load factor obtained from the analyses in -X and -Y are, indeed, equal to 0.55 g and 0.44g, respectively. It is observed that the structure is characterized by a lower capacity in +Y and +X directions with respect to -Y and -X directions, respectively. However, this can be attributed to the fact that the curves in +Y and +X directions were plotted for smaller ultimate displacements, as the curves almost coincide in the positive and negative directions.

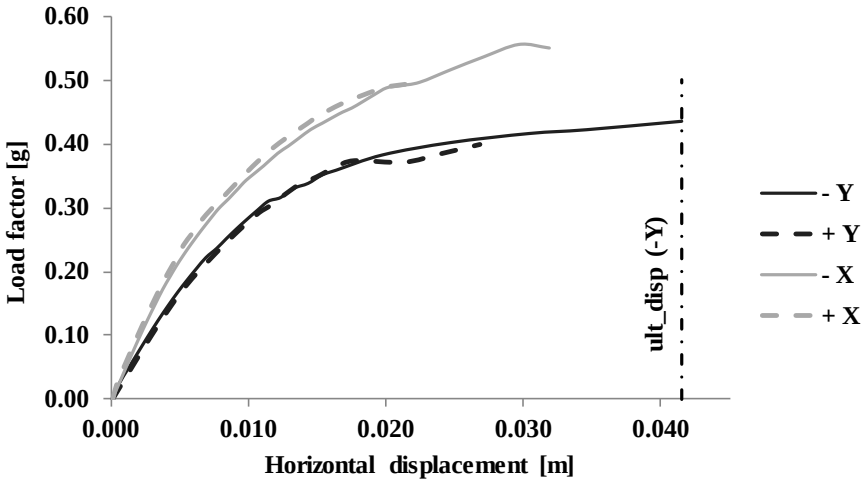

Figure 10 - Capacity curves obtained from the analyses performed in +X, -X, +Y and -Y directions.

Figure 11 presents the damage pattern of masonry walls in terms of principal crack width strain for the pushover analyses in -Y and -X direction, for which the maximum values of horizontal load factor were obtained. A global failure mechanism is observed in both the directions of analysis, with masonry walls mostly affected by diagonal shear cracks. Flexural cracks are also observed, especially in the spandrels. Furthermore, it is observed that, despite the higher values of horizontal load applied in -X direction, the damage is more severe in the analysis in -Y direction, as shown by damage distribution and higher values of principal crack width strain.

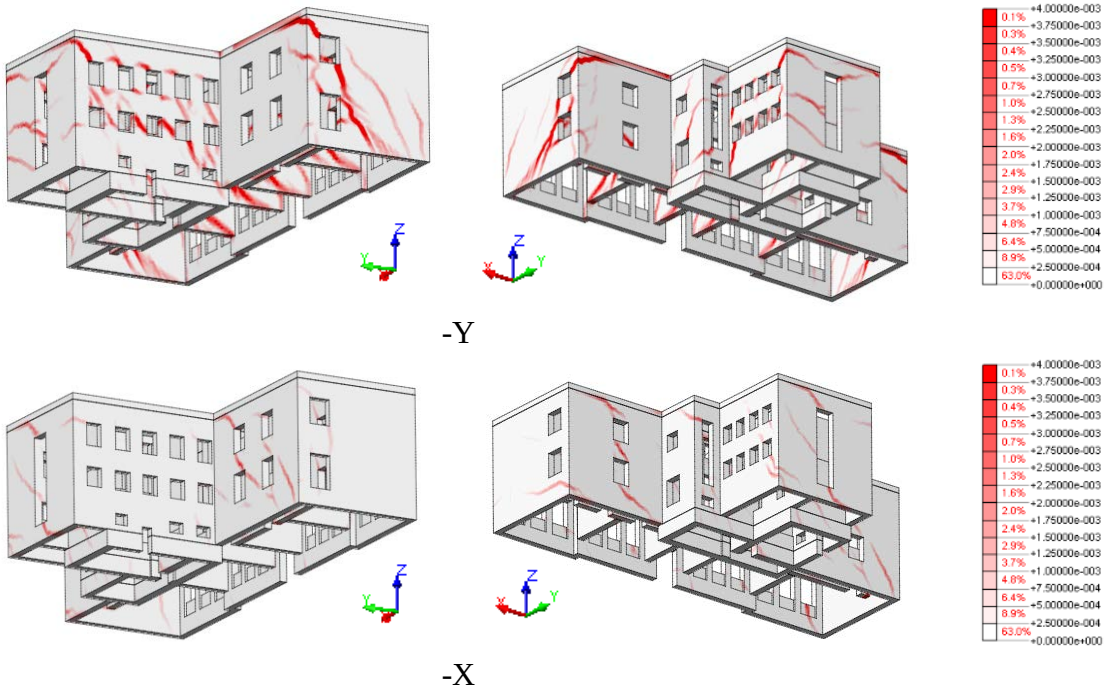

Figure 11 - Principal crack width strain for pushover analyses in -Y and -X directions.

Finally, even if pushover analyses are not able to fully represent the simultaneous action of an earthquake in different directions, a comparison can be attempted between the results obtained from pushover analyses and the seismic performance exhibited by the structure during the Amatrice-Visso-Norcia seismic sequence. According to the damage survey, “Pietro Capuzi” school was characterized by an in-plane response with severe cracks, mainly due to shear, in both internal and internal walls. Consequently, the damage mechanisms obtained from the numerical model are in good agreement with the crack pattern observed in the structure. As for the out-of-plane mechanism activated in one corner of the building after the seismic event of October 26th, 2016, it is to note that such a mechanism was difficult to obtain from the numerical model due to the presence of the concrete bond-beam at the top of the structure. Furthermore, it possibly resulted from a local disintegration of the material, which it is not considered in the FE model.

Regarding the seismic capacity, the maximum values of horizontal load that the structure was found to bear from pushover analysis are consistent with the values of PGA recorded during the seismic event of October 26th. In particular, this is clear in -Y direction where the maximum lateral load applied in the FE model was equal to 0.44 g and it was associated to a severe damage state compatible with the one observed in the building in the walls oriented in Y direction (Figure 12a). As for X direction, according to the results of pushover analyses, the building exhibited a higher seismic capacity, with a maximum lateral load equal to 0.55g, but

less severe damage. From Figure 12b, the PGA recorded in X direction was much lower and, indeed, the damage was less severe in X direction than in Y direction. In conclusion, the numerical model was found to accurately predict the seismic performance of the building in terms of horizontal maximum load and failure mechanisms.

(a) PGA_x = 0.36g (b) PGA_y = 0.47g

Figure 12 - Comparison between the damage distribution obtained in the walls oriented in X (a) and Y (b) after the Mw 5.9 earthquake of October 26th.

Conclusions

This paper presented the seismic assessment of “Pietro Capuzi” school in Visso, Marche, which was severely damaged by the 2016-2017 Amatrice-Visso-Norcia seismic sequence. First, the progressive damage suffered by the building after the subsequent earthquakes was analyzed in terms of development of the crack pattern and inter-storey drift. Secondly, on the basis of the documentation available in terms of geometry, construction details and material properties, a 3D macro FE model of the entire structure was prepared and calibrated according to the results of past identification dynamic tests. Finally, pushover analyses were performed in order to assess the seismic performance of the building. In both X and Y directions, the school exhibited a global in-plane response with cracks occurring in masonry piers and spandrels. A higher seismic capacity was observed in X direction with respect to Y direction. From the comparison between the numerical damage and the observed crack pattern, it was possible to conclude that the numerical model was capable to realistically simulate the seismic performance exhibited by the building during the past seismic events in terms of capacity to bear horizontal loads as well as failure mechanisms.

Acknowledgements

The authors are grateful to the Seismic Observatory of Structures, RELUIS and Ing. Serena Cattari of the University of Genova for the material made available for the development of the present work. Support was also provided by the SAHC Consortium and the University of Minho in Guimarães (Portugal).

References

[1] DPC Osservatorio Sismico delle Strutture OSS Download Service http://www.mot1.it/ossdownload, accessed 12/04/2017.

[2] S.G.M. S.r.l., *Rilievo geometrico e strutturale - Scuola elementare "Pietro Capuzi"- Visso (MC)*, 2010 (in Italian).

[3] S.G.M. S.r.l., *Rilievo proprietà meccaniche e rilievo geometrico costruttivo - Scuola elementare e materna “Pietro Capuzi” - Visso (MC)*, Relazione P4134-20/11, 2011 (in Italian).

[4] S.G.M. Engineering, *Modellazione e analisi numerica - Scuola elementare e materna "P. Capuzi" - Visso (MC*), 2011 (in Italian).

[5] CESI S.p.A., *Caratteristiche del sistema di monitoraggio sismico - Scuola materna "P. Capuzi", Visso (MC)*, Rapporto di installazione, 2010 (in Italian).

[6] Cattari, S., Degli Abbati, S., Ottonelli, D., Sivori D., Spacone, E., Camata, G., Marano, C., Da Porto, F., Lorenzoni, F., Penna, A., Graziotti, F., Ceravolo, R., Matta, E., Miraglia, G., Spina, D. and Fiorini, N., *Task 4.1 Workgroup_Report di sintesi sulle attività svolte sugli edifici in muratura monitorati dall'Osservatorio Sismico delle Strutture, Linea Strutture in Muratura*, ReLUIS report, Rete dei Laboratori Universitari di Ingegneria Sismica, 2017 (in Italian).

[7] Cattari, S. and Sivori, D. (2018) Lessons from the 2016 Central Italy Earthquakes: the seismic behavior of two masonry schools in Visso and Caldarola (Marche region), *Bulletin of Earthquake Engineering* (to be submitted).

[8] DPC, *Photographic survey performed during Amatrice-Norcia-Visso seismic sequence*, 2016.

[9] D.M. 14/1/2008, *Norme tecniche per le costruzioni (NTC 2008)*, Ministero delle Infrastrutture e dei Trasporti, 2008 (in Italian).

[10] DPC, Oss - *Osservatorio Sismico delle Strutture*, http://www.protezionecivile.gov.it/jcms/it/osservatorio.wp, accessed 12/04/2017.

[11] TNO DIANA BV, *DIANA Finite Element Analysis User's Manual Release 9.6*, Delft, The Netherlands, 2014.

[12] Lourenço, P. B., *Computational strategies for masonry structures*, PhD Thesis, Delft University of Technology, Netherlands, 1996.

[13] Silva, L. C., Mendes, N., Lourenço, P. B. and Ingham, J. (2018) Seismic Structural Assessment of the Christchurch Catholic Basilica, New Zealand, *Structures* **15**, 115-130.

[14] Circolare 2 febbraio 2009, n. 617, *Istruzioni per l'applicazione delle "Nuove norme tecniche per le costruzioni" di cui al decreto ministeriale 14 gennaio 2008*, 2009 (in Italian).

[15] Angelillo, M, Lourenço, P. B and Milani, G. (2014) *Masonry behaviour and modelling*, in Angelillo M (eds) Mechanics of Masonry Structures. CISM International Centre for Mechanical Sciences, vol 551. Springer, Vienna

[16] Lourenço, P. B., *A user/programmer's guide for the micro-modelling of masonry structures*. Relatório nº 03.21.1.31.35, Universidade Técnica de Delft, Delft, Países Baixos and Universidade do Minho, Guimarães, 1996.

[17] SVS, *ARTeMIS Modal, 5.0.0.1*, User's manual, Denmark, 2016.

[18] Ferrero, C., *2016 Central Italy Earthquake: Seismic Assessment of "Pietro Capuzi" School in Visso (Marche)*, SAHC Master Thesis, University of Minho, Guimarães, Portugal, 2017.

[19] Pastor, M, Binda, M. and Harcarik, T., Modal Assurance Criterion (2012) *Procedia Engineering* **48**, 543-548.

[20] Lourenço, P. B., Trujillo, A., Mendes, N. and Ramos, J. L., Seismic performance of the St. George of Latins church: Lessons learned from studying masonry ruins (2012) *Enginering Structure* ***40***, 501-518.